Monitoring eruptive activity at Mount St. Helens with TIR image data

R. G. Vaughan,[1] S. J. Hook,[1] M. S. Ramsey,[2] V. J. Realmuto,[1] and D. J. Schneider[3]

Received 19 July 2005; accepted 9 September 2005; published 14 October 2005.

[1] Thermal infrared (TIR) data from the MASTER airborne imaging spectrometer were acquired over Mount St. Helens in Sept and Oct, 2004, before and after the onset of recent eruptive activity. Pre-eruption data showed no measurable increase in surface temperatures before the first phreatic eruption on Oct 1. MASTER data acquired during the initial eruptive episode on Oct 14 showed maximum temperatures of ~330°C and TIR data acquired concurrently from a Forward Looking Infrared (FLIR) camera showed maximum temperatures ~675°C, in narrow (~1-m) fractures of molten rock on a new resurgent dome. MASTER and FLIR thermal flux calculations indicated a radiative cooling rate of ~714 J/m^2/s over the new dome, corresponding to a radiant power of ~24 MW. MASTER data indicated the new dome was dacitic in composition, and digital elevation data derived from LIDAR acquired concurrently with MASTER showed that the dome growth correlated with the areas of elevated temperatures. Low SO_2 concentrations in the plume combined with sub-optimal viewing conditions prohibited quantitative measurement of plume SO_2. The results demonstrate that airborne TIR data can provide information on the temperature of both the surface and plume and the composition of new lava during eruptive episodes. Given sufficient resources, the airborne instrumentation could be deployed rapidly to a newly-awakening volcano and provide a means for remote volcano monitoring. **Citation:** Vaughan, R. G., S. J. Hook, M. S. Ramsey, V. J. Realmuto, and D. J. Schneider (2005), Monitoring eruptive activity at Mount St. Helens with TIR image data, *Geophys. Res. Lett.*, *32*, L19305, doi:10.1029/2005GL024112.

1. Introduction

[2] Previous studies have demonstrated the utility of thermal infrared (TIR) remotely sensed data from airborne and spaceborne instruments for volcano monitoring [*Francis and Rothery*, 1987; *Realmuto et al.*, 1994; *Realmuto and Worden*, 2000; *Ramsey and Dehn*, 2004]. These studies show how TIR data can be used to determine the composition and temperature of the surface and plume. Because the data are acquired remotely they are relatively risk-free and can be used to look for precursor signals of increased volcanic activity. Unfortunately the only TIR satellite instruments that currently provide frequent (daily) coverage have low spatial resolution (1–8 km) and therefore considerable thermal activity needs to be underway to be detected; the higher spatial resolution satellite instruments (60–90 m) rarely acquire more than a few images per year over a given volcano. Airborne systems can provide higher spatial (<5 m) and temporal resolution measurements but cannot readily be used for global monitoring; however, with sufficient resources, airborne instruments can be rapidly deployed when increased activity is detected. Previously, no multispectral airborne TIR measurements had been acquired immediately prior and coincident with, the onset of volcanic activity. These data acquired at Mount St Helens (MSH) provide an opportunity to evaluate their potential for rapid-response volcano monitoring.

[3] On Sept 23, 2004 MSH began a new period of unrest with a swarm of shallow earthquakes. In the following weeks significant deformation of the crater floor was followed by several steam and ash eruptions and then extrusion of dacite lava accompanied by the formation and uplift of a new lava dome on the south side of the dome that formed from 1980–1986 following the large May 18, 1980 eruption [*Dzurisin et al.*, 2005]. During the period of unrest, several images of the volcano were acquired with the NASA MODIS/ASTER airborne simulator (MASTER) paired with a range-finding LIDAR, which allowed accurately georeferenced pixel elevation data to be linked with the MASTER data. Additionally, FLIR camera data were provided by the USGS Cascades Volcano Observatory (CVO), which deployed two FLIR cameras to collect both ground- and helicopter-based thermal images [*Schneider et al.*, 2004]. Table 1 lists the dates and times of various data acquisitions in chronological order together with the reported eruptive activity. These data were used to measure the surface temperature, radiant heat flux, and bulk composition of the new lava dome, and the amount of SO_2 degassing.

2. Data Acquisition and Processing

[4] MASTER is an airborne multispectral imager that measures radiance in 50 channels from the visible through TIR wavelengths [*Hook et al.*, 2001]. The 10 channels in the TIR range (7.8 to 12.9 μm) were used in this study. MASTER TIR at-sensor radiance data were atmospherically corrected to at-surface radiance using a radiative transfer model (MODTRAN 3.5) driven with atmospheric profiles obtained from the National Center for Environmental Prediction [*Hook et al.*, 2005]. Temperature and emissivity information were extracted from the at-surface radiance using the temperature-emissivity separation (TεS) method [*Gillespie et al.*, 1998; *Hook et al.*, 2005].

[5] Helicopter-based TIR data were acquired simultaneously with the MASTER overpass on Oct 14 using a FLIR Systems S-40 camera, which uses an uncooled microbolometer detector array to measure broadband

[1] Jet Propulsion Laboratory, Pasadena, California, USA.
[2] Department of Geology and Planetary Science, University of Pittsburgh, Pittsburgh, Pennsylvania, USA.
[3] Alaska Volcano Observatory, U.S. Geological Survey, Anchorage, Alaska, USA.

0094-8276/05/2005GL024112$05.00

Table 1. Chronology of Mount St. Helens Eruptive Activity and Remote Sensing Measurements

Date (2004)	Mt. St. Helens Activity	MASTER (5 m pixels)	FLIR Camera (0.4–1.4 m [H]) (3.1 m[a])	LIDAR (1 m pixels)
Sep 23	Seismic swarm begins			(Sep 2003)
Sep 24	Seismic activity continues, then wanes	4:30 pm		
Sep 30	Uplift south of old dome causing new fissures in glacial ice	1:30 pm		
Oct 1	First phreatic eruption		12:00–2:00 pm[b]	
Oct 2	Steam emission, Seismic tremor		8:00–10:00 am[b]	
Oct 4	Small steam eruption, large-scale dome uplift		9:00–10:00 am[b]	
Oct 11	First appearance of magmatic material at the surface		9:00–10:00 am[b]	
			2:20–3:40 pm[a]	
Oct 12	Steaming, lava extruding at the surface	8:00 am	7:20–8:20 am [b]	
			9:20–11:00 am[a]	
Oct 14	Steaming, lava extruding at the surface	8:00 am, 12:45 pm	8:00–9:15 am & 3:30–4:00 pm[b] 11:00–12:45 pm[a]	12:45 pm (w/MASTER)

[a]Measured using U. of Pittsburgh's FLIR with TIR telephoto lens from JRO.
[b]Measured using USGS helicopter-mounted FLIR.

radiance (7.5–14 μm) from the surface and convert that to at-surface temperature. A laser ranging instrument was used with GPS to calculate distance to the target and scale the FLIR pixel dimensions, typically sub-meter in size.

3. Results

[6] Figures 1a–1e show the dome temperatures (>30°C) retrieved from MASTER TIR data for each acquisition period, overlain onto LIDAR-generated shaded relief. MASTER-derived temperatures of a large fumarole (*fm* in Figure 1) range from 31 to 54°C. By comparison, a smaller area of this fumarole (~3.8 m^2) imaged by the University of Pittsburgh's handheld FLIR camera (with a telephoto 7° lens) revealed a maximum temperature of 50.2°C and an average of 43.6°C. The highest-temperatures on Oct 12 and Oct 14 show the spatial extent of the actively extruding lava on the west flank of the new dome. On Oct 14 the highest temperature measured by MASTER was 330°C and the highest temperature measured by the handheld FLIR camera from the same area was 675°C (in fractures and freshly broken surfaces). Although the spatial resolution of each measurement (5 m for MASTER, and < 1 m for FLIR) results in contrasting maximum temperature retrievals, the thermal flux calculated from each set of measurements is comparable. Thermal flux is a measure of the radiative cooling rate of an area and can be calculated from the Stefan-Boltzmann law:

$$\Phi = \sigma \varepsilon T^4 \quad (1)$$

where Φ is radiant flux ($J/m^2/s$), σ is the Stefan-Boltzmann constant (5.670×10^{-8} $J/K^4/m^2/s^1$), ε is emissivity, and T is temperature (K). From the MASTER data, the average temperature of the warmest areas (>30°C) of the new dome on Oct 14 (12:45 pm) was 70°C. Assuming an average emissivity of 0.91, this yields a thermal flux of 714 $J/m^2/s$. Over an area of 33,275 m^2, this corresponds to a power of ~24 MW. The radiant power over a similar area calculated from the FLIR temperatures on the same day was ~25 MW. The slight differences between these estimates are likely due to the differing spatial resolutions and viewing angles.

[7] Shaded relief images from a Sept 2003 LIDAR DEM approximate the topography of the dome on Sept 24 and Sept 30 (prior to the onset of eruption), and the LIDAR DEM from Oct 14, 2004 shows the dome topography for the last 3 acquisition periods (Figures 1a–1e). Figure 2 shows a 3-D perspective view of the temperature distribution on Oct 14, overlain onto the corresponding shaded relief image. The highest temperatures correspond to the location of an approximately 50 m high "fin-shaped" extrusion of fresh lava at the surface. Also, a small, hot block and ash flow is visible along the west flank of the new dome. Insets with Figure 2 are FLIR images from the same day that show (a) the extruding lava, (b) the large fumarole, and (c) the block and ash flow.

[8] The bulk composition of the new and old dome material was estimated by comparing spectral emissivity plots from these areas to reference spectra of dacite and andesite (Figure 3a). At an old dome site (Figure 3b) spectra

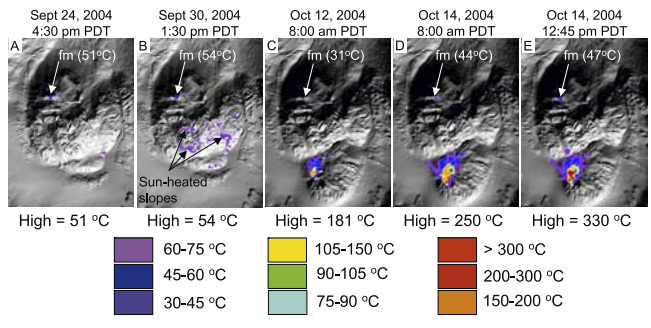

Figure 1. Mount St. Helens dome temperatures overlain onto LIDAR DEM shaded relief images. For Sept 24 and 30, the background images use LIDAR data acquired in 2003 to represent the pre-eruption/deformation topography; for Oct 12 and 14, the background images use LIDAR data acquired on Oct 14, 2004. For each image, north is up and the width is ~900 m.

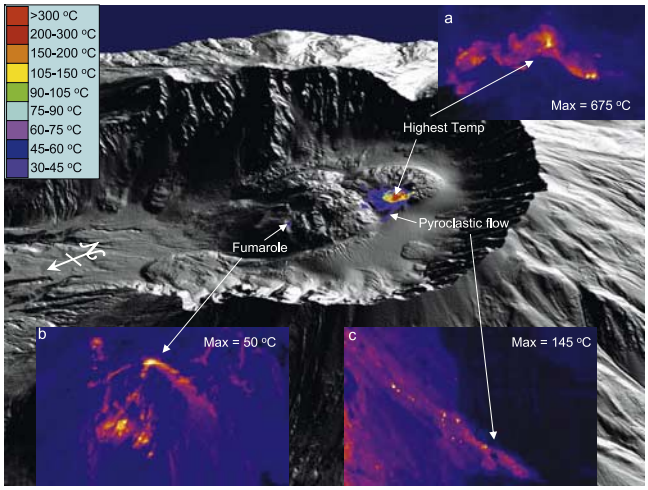

Figure 2. Mount St. Helens dome temperatures 3-D perspective view. MASTER temperature data from Oct 14, 2004 (5-m resolution) overlain onto a shaded relief image (1-m resolution – no vertical exaggeration) from LIDAR data acquired concurrently. The crater is ~2 km across. Inset images are from the handheld FLIR camera acquired from the USGS helicopter at the time of the MASTER over flight.

from Sept 24 and Oct 14 show a similar broad emissivity minimum at 9.0 and 9.7 μm, as does the spectrum retrieved from the new dome. These spectra are indicative of dacite, a finding later confirmed by petrographic analysis of new dome samples [*Dzurisin et al.*, 2005]. The broad spectral feature that occurs around 11 μm for each spectrum from Oct 14 may be due to the deposition of fine-grained volcanic ash that was widely distributed throughout the crater by Oct 14. Very fine-grained silicate minerals (<60 μm) are optically thin at the TIR wavelengths. As particle size decreases, scattered radiant energy increases at wavelengths around 11 μm, which causes an overall decrease in spectral contrast, [*Ramsey and Christensen*, 1998], and is consistent with the observed MASTER emissivity data.

[9] The MASTER flight on Oct 12 occurred near the end of a period of wet degassing from MSH, and the volcano emitted more H_2S than SO_2 [*Dzurisin et al.*, 2005]. The emission rates of SO_2 at that time were decreasing from the 70 tons per day reported by CVO on Oct 11. The estimation of SO_2 column abundance from multispectral TIR image data is based on the attenuation of ground radiance passing through a plume [*Realmuto et al.*, 1994]. The optimal conditions for this estimation technique occur when the plume temperature is lower than the ground temperature, and the plume is not opaque in the TIR. Figure 4a illustrates the MSH plume on the morning of Oct 12. According to CVO field observations, the plume was predominantly composed of steam and was free of ash (Figure 4a). A MASTER TIR brightness-temperature image (Figure 4b) indicates that much of the plume was opaque in the TIR. Within the crater the plume was ~3°C warmer (brighter) than the glacial material to the south of the dome. Near the crater rim the plume and ground were close to the same temperature, and the plume boundaries were hard to discern. Over the southern flank the plume was ~4°C cooler (darker) than the ground.

[10] Figure 4c shows the results of the SO_2 retrieval algorithm for a 425 meter-wide strip, oriented roughly perpendicular to the plume, over the southern flank of MSH. In general, the temperature contrast between the plume and ground was too low to detect SO_2 at the low levels reported by the CVO and the resulting SO_2 column abundance estimates were dominated by scan-line noise. The majority of the retrievals (55%) alternated between zero and 10 g/m^2, the upper limit set for the retrieval algorithm, and the probabilities for these values were approximately equal (29% for zero, 27% for 10 g/m^2). The probabilities for estimates between zero and 10 g/m^2 were all less than 0.5%, although the estimates less than 5 g/m^2 were generally an order of magnitude more likely than those greater than 5 g/m^2.

4. Summary and Conclusions

[11] On Oct 1, 2004 an eruption of steam and ash occurred on the south side of the resurgent dome inside the MSH crater. Neither anomalous gas emissions, nor thermal anomalies were detected in the week prior to this

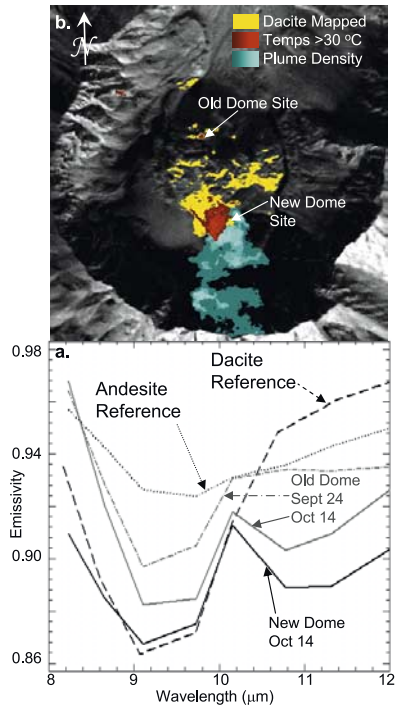

Figure 3. (a) MASTER spectral emissivity plots from both old dome (gray) and new dome (black) material are shown compared to reference spectra of dacite (dashed) and andesite (dotted). MASTER spectra from Oct 14 (solid) both show the effects of fine-grained ash covering the surface. The dacite reference spectrum from the ASTER spectral library (http://speclib.jpl.nasa.gov) is re-sampled to the MASTER spectral response functions; the andesite reference spectrum is from the spectral library of igneous rocks collected at the IVIS Laboratory (University of Pittsburgh). (b) Location of the areas from which spectra were extracted. Dacite was mapped based on its unique spectral features (yellow area); areas of elevated temperatures (>30°C) are shown in red gradient; and areas where the plume was optically thick are shown in blue gradient.

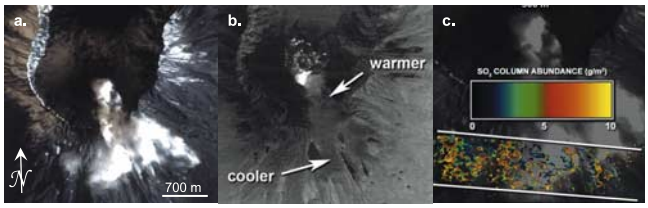

Figure 4. MASTER data acquired over Mount St. Helens on the morning of Oct 12, 2004. (a) True color composite of MASTER red, green, and blue image data. (b) Brightness temperature map generated from MASTER TIR data. Arrows indicate portions of the plume that were warmer (brighter) and cooler (darker) than the ground. (c) Map of SO_2 estimates generated by retrieval algorithm. Estimates of zero and 10 g/m^2 are transparent so that the intermediate values may be discerned.

initial eruption. Helicopter-based FLIR data acquired minutes prior to this eruption also did not show anomalous warming of the surface [*Schneider et al.*, 2004]; however, crevasses were seen forming in the glacier south of the old dome in the LIDAR data from Sept 30, indicating deformation. MASTER TIR data acquired during the subsequent period of lava extrusion were used to extract surface temperatures and estimate the bulk composition of the new lava. The temperatures were used to calculate thermal flux radiating from the new material and were consistent with flux calculations based on temperatures measured independently by a handheld FLIR instrument. Based on MASTER TIR spectral emissivity data both the new and old domes were interpreted as dacitic, consistent with field sample analyses [*Dzurisin et al.*, 2005].

[12] The attempt to estimate SO_2 column abundance with MASTER data demonstrates the interaction between temperature contrast and SO_2 concentration in the detection of SO_2 with TIR radiance measurements. Temperature contrasts in the 3–5°C range were not sufficient to detect low concentrations of SO_2. This lesson can be applied to future airborne campaigns, analyses of satellite data featuring low-contrast plumes, and design of sun-synchronous orbits for future spaceborne TIR instruments.

[13] The results demonstrate the value of multispectral TIR data for quantitatively measuring the heat budget of volcanic activity as well as compositional information about both new landforms and material released into the atmosphere. This study also highlights the potential advantages of a multi-sensor package for volcano monitoring: The combination of MASTER TIR data (from which temperature and emissivity of both the surface and plume can be measured), and LIDAR data (from which DEM and geolocation information can be derived) lead to improved visualization and interpretation of an evolving volcanic system (Animation 1). In general, airborne platforms provide higher spatial resolution images than can be achieved from satellites. Although these data were acquired in a fortuitously rapid response, this study demonstrates the value of developing a protocol for planned rapid response using multi-sensor airborne systems for volcano monitoring, hazard analysis and planning.

[14] **Acknowledgments.** The research described in this paper was carried out in part at the Jet Propulsion Laboratory, California Institute of Technology, under a contract with NASA as part of the Earth Observing System Mission to Planet Earth Program. Work by RGV was funded by a Caltech postdoctoral fellowship; work by MSR was partially supported by the NASA ASTER project and the NSF EAR-program. Additionally, we would like to thank the Airborne Sensor Group at Ames Research Center and everyone involved with the MASTER project; Ron Alley for help with MASTER data processing; Keith Howard and 1 anonymous reviewer for comments on this manuscript; Rick Wessels from the USGS AVO, who helped acquire some of the helicopter-based FLIR data during the first month of the volcanic crisis and was instrumental in bringing MSR and the U. Pitt. FLIR to MSH; and Jeff Byrnes for his help with the MASTER data processing. The USGS CVO is also thanked for providing the 2003 LIDAR data. Reference herein to any specific commercial product, process, or service by trade names, trademark, manufacturer or otherwise does not imply endorsement by the United States or the Jet Propulsion Laboratory, California Institute of Technology.

References

Dzurisin, D., J. W. Vallance, T. M. Gerlach, S. C. Moran, and S. D. Malone (2005), Mount St. Helens Reawakens, *Eos Trans. AGU*, *86*(3), 25–36.

Francis, P. W., and D. A. Rothery (1987), Using Landsat thematic mapper data to detect and monitor active volcanoes: an example from Lascar Volcano, northern Chile, *Geology*, *15*, 614–617.

Gillespie, A. R., S. Rokugawa, T. Matsunaga, J. S. Cothern, S. J. Hook, and A. B. Kahle (1998), A temperature and emissivity separation algorithm for Advanced Spaceborne Thermal Emission and Reflection Radiometer (ASTER) images, *IEEE Trans. on Geosci. Remote Sens.*, *36*, 1113–1126.

Hook, S. J., J. Myers, K. J. Thome, M. Fitzgerald, and A. B. Kahle (2001), The MODIS/ASTER Airborne Simulator (MASTER)—A new instrument for Earth science studies, *Remote Sens. Environ.*, *76*, 93–102.

Hook, S. J., J. E. Dmochowski, K. A. Howard, L. C. Rowan, K. E. Karlstrom, and J. M. Stock (2005), Mapping weight percent silica variation from remotely acquired multispectral thermal infrared data with examples from the Hiller Mountains, Nevada, USA and Tres Virgenes-La Reforma, Baja California Sur, Mexico, *Remote Sens. Environ.*, *95*, 273–289.

Ramsey, M. S., and P. R. Christensen (1998), Mineral abundance determination: Quantitative deconvolution of thermal emission spectra, *J. Geophys. Res.*, *103*, 577–596.

Ramsey, M. S., and J. Dehn (2004), Spaceborne observations of the 2000 Bezymianny, Kamchatka eruption: The integration of high-resolution ASTER data into near real-time monitoring using AVHRR, *J. Volcanol. Geothermal Res.*, *135*, 127–146.

Realmuto, V. J., and H. M. Worden (2000), The impact of atmospheric water vapor on the thermal infrared remote sensing of volcanic sulfur dioxide emissions: A case study from the Pu'u 'O'o vent of Kilauea Volcano, Hawaii, *J. Geophys. Res.*, *105*, 21,497–21,508.

Realmuto, V. J., M. J. Abrams, M. F. Buongiorno, and D. C. Pieri (1994), The use of multispectral thermal infrared image data to estimate the sulfur dioxide flux from volcanoes: A case study from Mount Etna, Sicily, July 29, 1986, *J. Geophys. Res.*, *99*, 481–488.

Schneider, D., R. Wessels, and M. S. Ramsey (2004), Airborne thermal infrared observations during the first month of the 2004 eruption of Mount St. Helens Volcano, Washington, *Eos Trans. AGU*, *85*(47), Fall Meet. Suppl., Abstract V31E-05.

S. J. Hook, V. J. Realmuto, and R. G. Vaughan, Jet Propulsion Laboratory, MS 183-501, 4800 Oak Grove Drive, Pasadena, CA 91109, USA. (simon.j.hook@jpl.nasa.gov; vincent.j.realmuto@jpl.nasa.gov; greg.vaughan@jpl.nasa.gov)

M. S. Ramsey, Department of Geology and Planetary Science, University of Pittsburgh, 200 SRCC Building, Pittsburgh, PA 15260, USA. (ramsey@ivis.eps.pitt.edu)

D. J. Schneider, Alaska Volcano Observatory, U.S. Geological Survey, Anchorage, AK 99508, USA. (djschneider@usgs.gov)